

Appropriate numerical conditions for practical LES of actual high rise building -Requirement of grid number and wind direction-

H. Kawai¹, T. Tamura¹, Y. Ono², K. Kondo³, H. Kikuchi⁴ and K. Otake⁵

¹Department of Architecture and Building Engineering
Tokyo Institute of Technology, Yokohama, Kanagawa, 226-8502, Japan

²Technical Research Institute,
Obayashi Corporation, Kiyose, Tokyo, 204-0011, Japan

³Kajima Technical Research Institute,
Kajima Corporation, Chofu, Tokyo, 182-0036, Japan

⁴Institute of Technology,
Shimizu Corporation, Koto-ku, Tokyo, 135-0044, Japan

⁵Takenaka Research & Development Institute,
Takenaka Corporation, Inzai, Chiba, 270-1395, Japan

Abstract

For estimation of wind load by CFD, number of inflow wind direction, ensemble number, and integration time increase calculation loads. Thus, practical method is necessary for CFD. This study clarifies the accuracy of wind pressure in LES at reduced grid number. As a result, peak wind pressure coefficient underestimated at the lower part, corner and roof of high rise building, but the tendency of local wind pressure and force on target building is reproduced in the case at reduced grid number. Next, evaluation of maximum and minimum C_p value for design ($C_{p_{x,D_MAX}}$, $C_{p_{x,D_MIN}}$) by reduced wind direction number is examined. As a result, The possibility to estimate $C_{p_{x,D_MAX}}$, $C_{p_{x,D_MIN}}$ assuming 20% difference is shown in reduced wind direction number (18,36 directions).

Introduction

In the current stage of CFD techniques, high performance computing has developed distinctly, so high-resolution and large-domain computation becomes possible for flows over complicated configuration such as urban covering surfaces. Many CFD techniques almost have reached the feasibility level for providing the aerodynamic data to design of buildings, comparable to the data obtained by wind tunnel experiment. In Japan, "Wind-induced response and Load Estimation/Practical Guide of CFD for Wind Resistance Design"[1] was issued by Architectural Institute of Japan (AIJ). Also, some researchers show wind load estimation of actual building with complicated shape. For example, Yoshikawa et. al [2] analyses the effect of turbulent flow generated from upwind building for wind load estimation by using Large Eddy Simulation (LES). Yoshikawa et.al [3] reveals the relation between turbulent field around the vertical claddings and wind load by LES. In addition, Kawai and Tamura [4] shows high resolution LES for the wind load for high rise buildings with claddings by using K supercomputer.

On the other hand, most of these simulations require large calculation resource because a large number of grids are necessary to reproduce velocity and pressure field around complicated geometry such as claddings. Also, number of wind direction of inflow increases calculation cost for estimation of wind load by CFD.

This study clarifies the accuracy of wind pressure in LES at reduced grid number for actual buildings. Then, the dependency on inflow wind direction for wind load estimation of high rise buildings with claddings is examined.

Target case and Methodology

Target case

This study focuses on two target case (Fig. 1). One is a high rise residential building (Height 128m, Breadth 43m) located in urban districts. This building has a balcony at each floor. Also, the upper floors have the plan with double recessed corner and chamfered corner. The other is office building with eaves for solar shading (Height 128m, Breadth 50m). The office building has crown wall on the roof and void in lower part. In target cases, surrounding buildings is reproduced within a 400-meter radius from the target building.

Wind tunnel experiment

In wind tunnel experiment, the surface pressure on target building and the profile of velocity for 72 inflow wind directions are measured. The time series of surface pressure on target building is obtained at sampling frequency of 1000Hz (Sampling number: 65536) by multipoint simultaneous measurement technique. For measurement of velocity, X-type hot wire anemometer is used. Target building and surrounding buildings is

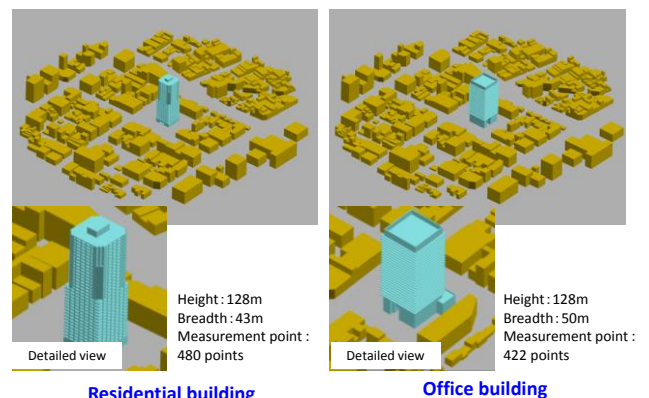


Figure 1. Target building

reproduced at a scale of 1/400 on turn table (Radius:1m). 10m/s is assumed as inflow velocity at a top height of target building (0.32m: model scale). In this study, in order to obtain reliable data, same experiments is carried out in the 3 facilities by using same model, and their results are compared. In addition, the effect of ensemble number for averaging on the statistic value is confirmed by comparing the data averaged at 1-9 ensemble numbers. Fig. 2 shows the vertical profile of streamwise velocity component at a leeward point from the center of turn table. The averaged velocity and turbulent intensities obtained from 3 facilities correspond to that in category III of AIJ recommendation. Then, at the point at the top height of target building, turbulent length scale of facility A is larger than that of facility B, C.

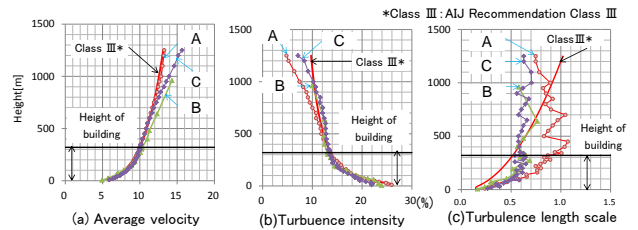


Figure 2. Inflow vertical profile of wind tunnel experiment

Numerical simulation method

In this study, grid dependencies are examined in two type of buildings and wind directions. Table 1 shows calculation case. Cases where inflow wind direction is 80, 65 degree are examined because previous research shows occurrence of large negative pressure in the corner of building.

Numerical simulation is implemented at the same scale as wind tunnel experiment (1:400). 10 minutes of evaluation duration in real building scale is corresponding to 6.735s. The governing equation is the incompressible Navier-Stokes equation (Eq. (1)) and continuity equation (Eq. (2)).

$$\nabla \cdot \mathbf{u} = 0 \quad (1)$$

$$\frac{\partial \mathbf{u}}{\partial t} + \nabla \cdot (\mathbf{u}\mathbf{u}) = -\frac{1}{\rho} \nabla p + \nu \nabla^2 \mathbf{u} + \mathbf{f} \quad (2)$$

The detailed calculation condition is shown in Table 2. To solve the advection term, the second-order central-difference scheme is used. To perform time integration, the euler implicit scheme is used; the numerical algorithm is based on the SMAC method. Time increment is $dt=1.0 \times 10^{-4}$ [s]. The flow and pressure field is solved by using Frontflow/Red-HPC edition (FFR-HPC). For discretization of equations, finite volume method by unstructured grid is used. All variables are defined at the vertex center in the collocated grid. Boundary condition is shown in table 3.

Figure3 and Table4 show distribution of grid. Configuration of surrounding building and distribution are common in two type building (Office building and residential building). In this study, 8 regions of vol1~vol8 are defined by grid resolution level and grid resolution in each grid resolution level is determined respectively in 200 million grid case and 50 million grid case (Table 1). Minimum size of tetra element is 0.4m in 200 million grid case and 0.6m in 50 million grid case.

Effect of Grid Resolution on the Estimation of Wind Pressure

Office building

Figure 4 shows the correlation between the cases with different grid number (OF90_200M-OF90_50M, OF65_200M-OF65_50M). Average pressure coefficient and fluctuation pressure coefficient in OF90_50M and OF65_50M are within 20% difference from them of OF90_200M and OF65_200M almost all points. On the other hand, for maximum and minimum of pressure coefficient (C_{pmax} , C_{pmin}), difference between 200 million and 50million mesh cases exceeds 20% in some points located in crown wall, eaves between 26F and 27F, and lower part less than 5F. However, tendencies of C_{pmin} and C_{pmax} in 50million mesh cases correspond to them in 50million mesh cases.

Table 1. Calculation case

Case	Building	Wind direction	Grid number
OF90_50M	Office	90°	50 million
OF65_50M	Office	65°	50 million
RS90_50M	Residential	90°	55 million
RS80_50M	Residential	80°	55 million
OF90_200M	Office	90°	210 million
OF65_200M	Office	65°	210 million
RS90_200M	Residential	90°	250 million
RS80_200M	Residential	80°	250 million

Table 2. Calculation method

Grid system	Vertex centered grid
Algorithm	SMAC method
Time integration	Euler implicit
Spatial discretization	2 nd order central difference
Numerical viscosity	5% 1 st order upwind difference (blended in partial region)
SGS model	Smagorinsky Model ($C_s=0.12$)

Table 3. Boundary conditions

Inflow	Velocity	Dirichlet(Velocity vector of inflow turbulence)
	Pressure	Neumann
	Corrected pressure	Dirichlet($P'=0$)
Outflow	Velocity	Neumann
	Pressure	Neumann
	Corrected pressure	Dirichlet ($P'=0$)
Side	Free-Slip	
Top	Free-Slip	
Wall	Wall function (Spalding law)	

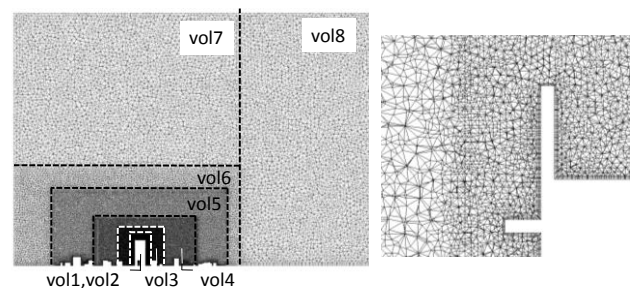


Figure.3 Example of definition of grid distribution (OF65_50M)

Table 4. Grid size in each volume
(a)200 million grid case

	Surface	Tetra Element	Thickness of boundary
vol1	0.3m	0.4m	0.06m
vol2	0.5m	0.5m	0.1m
vol3	1m	1.1m	0.2m
vol4	2m	2.2m	0.3m
vol5	2m	3.5m	0.3m*
vol6	10m	12m	2m*
vol7	20m	20m	-
vol8	30m	30m	6m*

* Applied to only ground

(b) 50 million grid case

	Surface	Tetra Element	Thickness of boundary
vol1	0.45m	0.6m	0.09m
vol2	0.75m	1.1m	0.15m
vol3	1.5m	2.4m	0.3m
vol4	3m	4.4m	0.45m
vol5	3m	6.9m	0.45m*
vol6	10m	12m	2m*
vol7	20m	20m	-
vol8	30m	30m	6m*

* Applied to only ground

Residential building

Figure 5 shows the correlation between the cases with different grid number (RS90_200M-RS90_50M, RS80_200M-RS80_50M). Average pressure coefficient and fluctuation pressure coefficient in RS90_50M and RS80_50M are within 20% difference from them of RS90_200M and RS80_200M almost all points. For maximum of pressure coefficient, though difference between 200 million and 50million mesh cases is within 20% in points where its C_{pmax} value is more than 1.0, difference between 200 million and 50million mesh cases exceeds 20% in some points located in roof and lower part less than 11F.

Effect of Wind Direction Number on the Estimation of Wind Pressure

In order to examine the wind direction number for practical evaluation of wind resistance design by LES, this study shows the effect of wind direction number on maximum C_p value for design ($C_{p_{xD_MAX}}$) and minimum C_p value for design ($C_{p_{xD_MIN}}$). In this study, maximum C_p value for design ($C_{p_{xD_MAX}}$) is defined as the maximum of maximum C_p in x directions at a probe point and minimum C_p value for design ($C_{p_{xD_MIN}}$) is also defined as the minimum of minimum C_p in x directions at a probe point.

Spatial distributions of maximum and minimum C_p for design

Spatial distributions of maximum and minimum C_p for design ($C_{p_{72D_MAX}}$, $C_{p_{72D_MIN}}$) and wind directions, where $C_{p_{max}}$, $C_{p_{min}}$ is equal to $C_{p_{72D_MAX}}$, $C_{p_{72D_MIN}}$ respectively, are shown in figures 7(a), 8(a). Variations of $C_{p_{max}}$, $C_{p_{min}}$ in 72 wind directions in extracted points are shown in 7(b), 8(b). First, focusing on the center of wall (point 125 in fig.7 (b) and point 298 in fig. 8 (b)), C_{pmax} is equal to $C_{p_{72D_MAX}}$ in perpendicular direction to wall in both office and residential buildings. At the corner of wall (123, 128 points in fig.7 (b) and points 295, 301 in fig. 8 (b)), wind directions where $C_{p_{max}}$ is equal to $C_{p_{72D_MAX}}$ are moved to approximately 30° inclined direction from perpendicular direction to wall. On the other hand, $C_{p_{72D_MAX}}$ value is similar to the value at the center points, and spatial distribution of $C_{p_{72D_MAX}}$ is almost uniform in the points at the same height.

Next, for minimum C_p value for design ($C_{p_{72D_MIN}}$), at the center points on wall, $C_{p_{72D_MIN}}$ value appears in parallel direction to wall. At the corner points in residential building (points 123 in fig 7(b)), $C_{p_{72D_MIN}}$ value appears in a slightly inclined direction from the parallel direction to wall, and the absolute value of $C_{p_{72D_MIN}}$ becomes larger than that at the center and other points. This tendency is corresponding to the previous research (Miyagi et. al[5]) which discusses the minimum C_p peak value at the slightly-inclined wind direction called as “glancing angle”. On the other hands, at the corner points (points 295 in fig 8(b)), $C_{p_{72D_MIN}}$ value appears in about 180° different angle from that at the corner point of residential building. This is because wind flows through the void space which penetrates lower floors. Reverse flows which are induced by flows from the void cause separation at the leeward corner (fig. 9).

Evaluation of $C_{p_{xD_MAX}}$, $C_{p_{xD_MIN}}$ by reduced wind direction number

The effect of wind direction number on maximum and minimum C_p value for design $C_{p_{xD_MAX}}$, $C_{p_{xD_MIN}}$ is shown in fig. 10. Even in the case where the number of direction is reduced to 18 directions, the difference of from 72 directions case $C_{p_{xD_MAX}}$, $C_{p_{xD_MIN}}$ is within 20%. Then, fig. 11 shows the variation of $C_{p_{max}}$ and $C_{p_{min}}$ in 72, 36, 18 wind directions. $C_{p_{max}}$ and $C_{p_{min}}$ changes continuously with corresponding to change of wind direction.

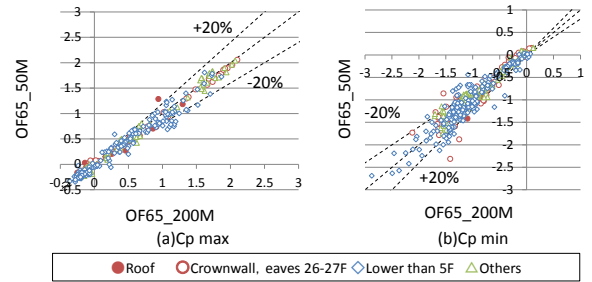


Figure.4 C_p correlation between OF65_50M and OF65_200M

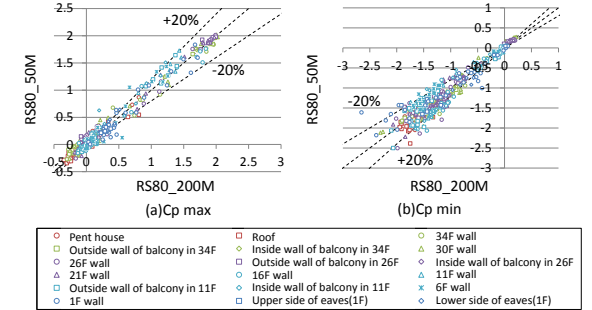
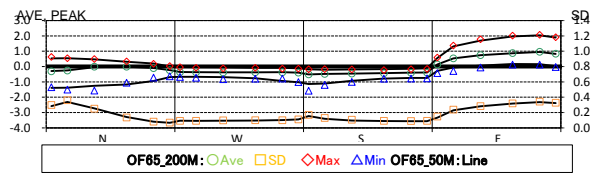
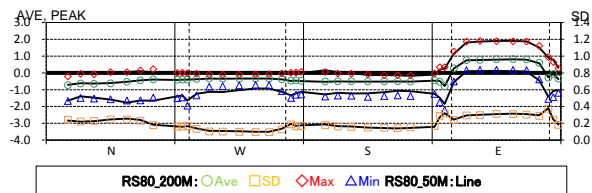


Figure.5 C_p correlation between RS80_50M and RS80_200M

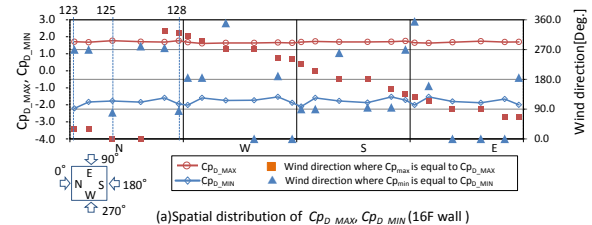


(a) 26F wall (Office building, 65deg.) (z=115.5m)

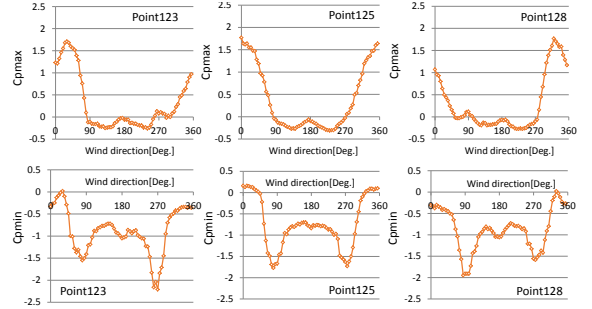


(b) 21F wall (Residential building, 80 deg.) (z=76.7m)

Figure.6 C_p distribution on walls in office building and residential building



(a) Spatial distribution of C_{pD_MAX} , C_{pD_MIN} (16F wall)



(b) Wind direction dependency of $C_{p_{max}}$, $C_{p_{min}}$ (in each point)

Figure.7 Spatial distributions of maximum and minimum C_p ($C_{p_{72D_MAX}}$, $C_{p_{72D_MIN}}$) for design (residential building)

Also, when evaluating $C_{p_{xD_MAX}}$, $C_{p_{xD_MIN}}$ in reduced 36, 18 wind directions, wind direction where $C_{p_{max}}$ and $C_{p_{min}}$ is equal to $C_{p_{xD_MAX}}$, $C_{p_{xD_MIN}}$ is different from that in 72 directions within the range of 10 degrees.

Taking the above discussion into consideration, The possibility to estimate $C_{p_{xD_MAX}}$, $C_{p_{xD_MIN}}$ assuming 20% difference is shown in reduced wind direction number (18,36 directions).

Conclusions

This study clarifies the accuracy of wind pressure in LES at reduced grid number. As a result, difference exceeding 20% in peak wind pressure coefficient appears at the lower part, corner and roof of high rise building, but the tendency of local wind pressure and force on target building is reproduced in the case at reduced grid number.

Next, estimation of maximum and minimum C_p value for design ($C_{p_{xD_MAX}}$, $C_{p_{xD_MIN}}$) when wind direction number is reduced is shown and compared with the estimation results by 72 wind directions. The results shows that the difference of from 72 directions case $C_{p_{xD_MAX}}$, $C_{p_{xD_MIN}}$ is within 20% and $C_{p_{max}}$ and $C_{p_{min}}$ changes continuously for each wind directions. Finally, the possibility to estimate $C_{p_{xD_MAX}}$, $C_{p_{xD_MIN}}$ assuming 20% difference is shown in reduced wind direction number.

Acknowledgments

This research is implemented by the project of Building Standard Development Promotion Program funded by MILT. This research used computational resources of the K computer provided by the RIKEN Advanced Institute for Computational Science through the HPCI System Research project (Project ID:hp160248).

References

- [1] Architectural Institute of Japan: Wind-induced response and Load Estimation/Practical Guide of CFD for Wind Resistance Design,2017
- [2] Yoshikawa, M., Tamura, T.:Evaluation of fluctuating wind pressures on 3D square cylinder by unstructured-grid LES – Formulation of LES using unstructured grid system for wind resistant design of buildings (Part1)- J.Struct. Constr. Eng.,AIJ,No.687,913-921,2013 (In Japanese)
- [3] Yoshikawa, M., Tamura,T., CFD Wind-resistant Design of Tall Building in Actual Urban Area Using Unstructured-grid LES, IABSE2015,1-8,2015
- [4] Tamura T., Kondo K., Kataoka H. and Kawai H., Estimation of wind estimation of wind loads on actual building by computational fluid dynamics, The proceedings of 24th national symposium on wind engineering, 253-258, 2016 (In Japanese)
- [5] Tetsuro T. and Miyagi, T., The effects of corner shape on aero dynamic characteristics of a type of square cylinder, J.Struct. Constr. Eng.,AIJ, No.514,51-58,1998 (In Japanese)

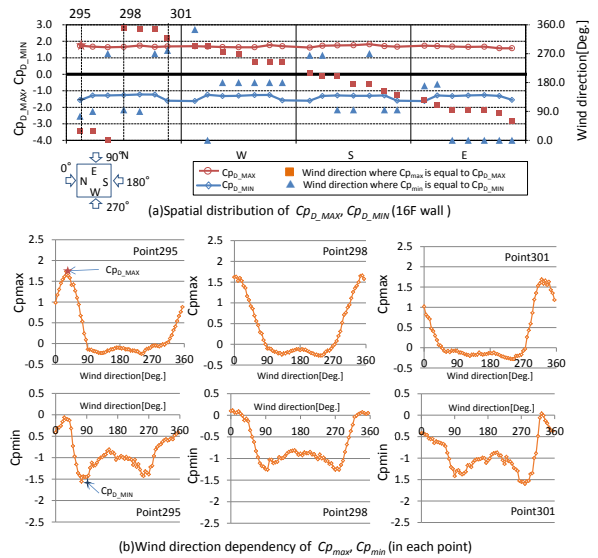


Figure.8 Spatial distributions of maximum and minimum $C_p(C_{p_{72D_MAX}}$, $C_{p_{72D_MIN}}$) for design (Office building)

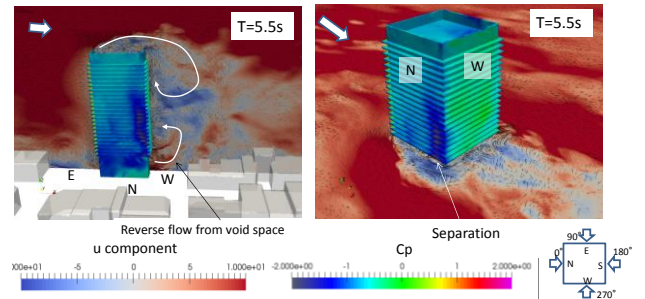


Figure.9 Spatial distributions of C_p and velocity (Office building)

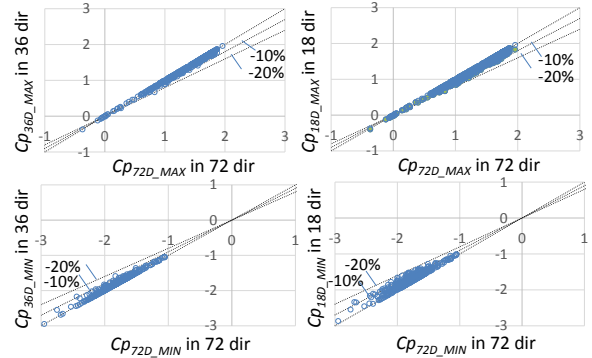


Figure.10 $C_{p_{xD_MAX}}$ and $C_{p_{xD_MIN}}$ correlation between the cases in 72, 36 and 18 wind directions (Office building)

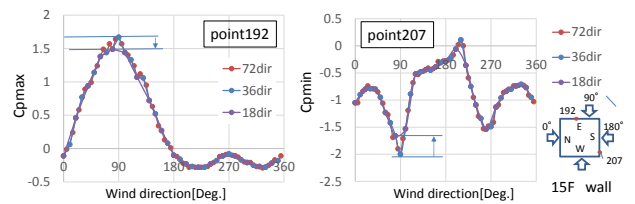


Figure.11 Variation of C_{pmax} and C_{pmin} for 72, 36 and 18 wind directions (Office building)